Simulations of global evapotranspiration using semiempirical and mechanistic schemes of plant hydrology

Simulations of global evapotranspiration using semiempirical and mechanistic schemes of plant hydrology

Paul Alton,[1] Rosie Fisher,[2] Sietse Los,[1] and Mathew Williams[3]

Received 9 April 2009; revised 22 June 2009; accepted 29 July 2009; published 13 November 2009.

[1] Some of the plant hydrology schemes implemented in global land surface models (LSMs) are relatively simple. This is despite evidence that simulated carbon, water, and energy fluxes are sensitive to both the availability of soil moisture and the formulation of plant hydrology. The current study introduces a mechanistic scheme of plant hydrology (soil-plant-atmosphere (SPA)) into a global LSM (Joint U.K. Land Environmental Simulator (JULES)) in order to compare with a traditional, semiempirical plant hydrology scheme (SiB) based on the Ball-Berry stomatal relation. The SPA scheme simulates explicitly the physical processes which change leaf water potential and account for the flow of water through the soil-plant-atmosphere media. Using both plant hydrology schemes, the annually averaged global evaporation-to-precipitation ratio is 0.58±0.9. The annually averaged global transpiration-to-precipitation ratio is 0.22±0.09 and 0.28±0.08 using the SPA and SiB plant hydrology schemes, respectively. The output from the two plant hydrology schemes typically differs less than the systematic errors associated with the different observational data sets (eddy covariance fluxes, continental runoff, etc.) employed to calibrate and validate the LSM. However, SPA is more conservative with respect to plant water use efficiency compared to SiB. This is partly due to the exhaustion of stored leaf water (not accounted for with the SiB scheme) which acts to limit afternoon transpiration when diurnal vapor pressure deficit is greatest. The trend in global runoff simulated with both plant hydrology schemes for the latter half of the 20th century (−1% per 50 years) agrees well with recent observational estimates that sample 80% of the global runoff network.

Citation: Alton, P., R. Fisher, S. Los, and M. Williams (2009), Simulations of global evapotranspiration using semiempirical and mechanistic schemes of plant hydrology, *Global Biogeochem. Cycles*, *23*, GB4023, doi:10.1029/2009GB003540.

1. Introduction

[2] The latent heat (LE) release from the land surface has a large impact on climate in terms of energy and water exchange [*Sellers et al.*, 1997]. Plants play a major role in this process through the release of water vapor through their stomata i.e. via transpiration (TR). Despite its importance to the water balance, estimates of regional evapotranspiration (ET) presented in the literature are usually inferred by subtraction of runoff from precipitation (PPT) [*Eltahir and Bras*, 1996; *Fisher et al.*, 2008]. Exceptions include isotope measurements conducted in the Amazonian basin [*Salati et al.*, 1979; *Gat and Matsui*, 1991] and simple source/sinks models based on measured atmospheric moisture [*Brubaker et al.*, 1993; *Eltahir and Bras*, 1996]. Estimates of regional or global ET, based on a bottom-up approach that simulates surface evaporation and plant transpiration, are still relatively scarce [*Trenberth et al.*, 2007].

[3] With regards to the calculation of TR, a variety of plant hydrological models are implemented in land surface models (LSMs) [e.g., *Hunt et al.*, 1991; *Sellers et al.*, 1996a, 1996b; *Cox et al.*, 1999; *Hickler et al.*, 2006; *Fisher et al.*, 2008]. Some of those implemented in global models are relatively simple, partly for reasons of computational efficiency. This is despite many global simulations manifesting a high sensitivity to both the availability of soil moisture [e.g., *Dai and Fung*, 1993; *Tian et al.*, 1998; *Nemani et al.*, 2002; *Peylin et al.*, 2005] and the formulation of plant hydrology [e.g., *Knorr and Heimann*, 2001]. Furthermore, a hitherto major focus for global land surface simulations is carbon balance and how the terrestrial biosphere will react to increasing atmospheric CO_2 concentration [*Cramer et al.*, 2001; *Knorr and Heimann*, 2001; *Friend et al.*, 2007]. It is only relatively recently that global LSMs are being evaluated in terms of simulated water balance [*Gordon et al.*, 2004; *Fisher et al.*, 2008], although carbon and water exchange are closely linked [*Sellers et al.*, 1997].

[4] The present study calculates global ET and TR by implementing two state-of-the-art plant hydrology schemes into a land surface model. The first scheme is a semiem-

[1]Geography Department, Swansea University, Swansea, UK.
[2]Department of Animal and Plant Sciences, University of Sheffield, Sheffield, UK.
[3]School of Geosciences, University of Edinburgh, Edinburgh, UK.

0886-6236/09/2009GB003540

pirical approach which is traditionally adopted in many global land surface simulations. The second scheme represents a more mechanistic approach which simulates explicitly (i.e. through well defined physical processes) the flow of water through the soil-plant-atmosphere media. This is the first time that this mechanistic scheme is implemented in a global simulation. The main scientific aims of the current investigation are summarized as follows: (1) to quantify the global distribution of ET and TR and to ascertain how these quantities vary according to vegetation type and climatic zone; (2) to gauge uncertainties in estimating global TR and ET through the implementation of different representations of plant hydrology; (3) to determine whether a mechanistic plant hydrology scheme confers greater skill in predicting site-level and regional water balance; and (4) to test the success with which a LSM calibrated at site level can predict global land surface water balance under both current climate and recent climatic change.

2. Methods and Materials

[5] The methodology, discussed in detail below, consists of 3 phases conducted separately for each plant hydrology scheme: (1) the calibration and validation of the LSM at site level using eddy covariance fluxes in the Marconi FLUXNET archive; (2) a global simulation of ET and TR conducted under current (recent) climate, analyzed with respect to latitude and Plant Functional Type (PFT) and validated against measurements of regional ET and runoff; and (3) a global simulation conducted for the latter half of the 20th century under increasing atmospheric CO_2 concentration.

2.1. Data Sets

[6] To calibrate and test the LSM at site level we use the observed half-hourly fluxes and tower-based meteorology contained in the Marconi FLUXNET archive [*Baldocchi et al.*, 2001; *Falge et al.*, 2002]. In order to simulate ET, we require a complete tower-based meteorology throughout the growing season in order to drive the LSM. In all, 30 sites fit this condition, yielding a total of 71 site years (Table 1 of Text S1).[1] For the purposes of calibration, each site year is ascribed to one of five PFTs defined within the model, namely: broadleaf trees (BL), needleleaf trees (NL), C_3 grassland (C_3), C_4 grassland (C_4) and shrubs (SH). For each site year, we follow *Lloyd et al.* [2002] in deriving GPP as $F+\Delta C+R_e$, where F is the downward carbon flow recorded above the canopy, ΔC is the CO_2 storage term and R_e is the ecosystem respiration. R_e is estimated from nighttime carbon flow (GPP=0) under moderate airflow [*Medlyn et al.*, 2003] using a linear function of soil temperature. Model and observations are only compared over the growing season (generally Day of Year 130–255) since it is the transpirational component of ET that is likely to differ the most between the two implementations of plant hydrology. Furthermore, we require a frictional velocity >0.16 ms^{-1} [*Reichstein et al.*, 2003] or a windspeed >2 ms^{-1} [*Medlyn et al.*, 2003] to ensure that measured fluxes are not severely underestimated [*Goulden et al.*, 1996]. Measured and simulated LE are converted to ET and integrated ET is scaled according to the number of rejected LE fluxes ($\simeq 30\%$) to provide realistic estimates of growing season ET. In addition to observed carbon and LE fluxes, the Marconi database provides the half-hourly meteorology required to force the LSM at site level (phase 1).

[7] Global LSMs contain many biophysical parameters and still no consensus exists as to the best way to calibrate such models. Both *Wang et al.* [2001] and *Medlyn et al.* [2005] caution that only a limited number of parameters are tuneable ($\simeq 3$) owing to parameter and flux interdependencies. In contrast, *Friend et al.* [1997] advocate average field measurements for the assignment of biophysical parameters and this approach is adopted by *Zaehle et al.* [2005]. The current investigation makes a compromise between parameter-tuning and measurement-based calibration. A previous sensitivity analysis of the LSM used in the current investigation indicates that the photosynthetic capacity at the top of the plant canopy ($V_{c\max}$) is the most important parameter for accurate predictions of both carbon and water exchange [*Alton et al.*, 2007a]. This finding accords with a growing number of studies which indicate that photosynthetic capacity is highly influential in LSMs which use a biochemical model to estimate canopy photosynthesis [*Dang et al.*, 1998; *Wang et al.*, 2001; *Reichstein et al.*, 2003]. Therefore, we calibrate the LSM separately for each site year in the Marconi archive via optimization of $V_{c\max}$. Optimized values of $V_{c\max}$ are inferred from a least squares minimization of simulated GPP against Marconi-derived GPP for half-hourly intervals over the growing season. All other biophysical parameters, including those influencing plant hydrology, are extracted from average field measurements within the literature (as discussed below). For the global simulation, each PFT is parameterized by median averaging the optimized values of $V_{c\max}$ across all relevant Marconi site years. The LSM does not calculate LAI and the phenology for the simulations is provided by the 10 day satellite-derived LAI time series of *Los et al.* [2000] at a spatial resolution of 0.25° and 1° for the site-level and global simulations, respectively. For the site simulations we normalize the peak LAI of the time series to the maximum LAI recorded in situ [*Law et al.*, 2002] in order to account for sub-grid-scale heterogeneity.

[8] The performance of the LSM at site level is evaluated by comparing simulated and measured ET. This is done using both a separate calibration of $V_{c\max}$ for each individual site year and a median calibration of $V_{c\max}$ for each PFT, the latter as adopted in the global simulation. Simulated site-level TR for the growing season is also compared against estimates derived from below-canopy eddy-covariance fluxes [*Law et al.*, 2002] and scaling of sap flow [*Granier et al.*, 2000; *Lundblad and Lindroth*, 2002] for 6 temperate and boreal forest stands. Direct measurements of TR for the Marconi sites are still fairly scarce in the literature but such methods are an important current focus at FLUXNET sites [e.g., *Fisher et al.*, 2007].

[9] For the global simulations under current climate (phase 2), we adopt the 3-hourly meteorological forcing of the Global Soil Wetness Project (GSWP2) [*Dirmeyer et*

[1] Auxiliary materials are available in the HTML. doi:10.1029/2009GB003540.

al., 1999] for the 10 year period 1986–1995. Preliminary testing indicates a convergence in initial soil moisture within the LSM after a spin-up of 2–3 years. Thus, years 1986–1988 (incl.) from the GSWP serve as spin-up for the LSM for both the site and global simulations. For the latter simulations, model output from the last 7 years is averaged to provide the global distribution of annual GPP, ET and TR at a spatial scale of 1°. Zonal estimates are compared against ET and runoff inferred from measured river discharge [*Baumgartner and Reichel*, 1975; *Henning*, 1989; *Cogley*, 2003]. Uncertainties in the global predictions are estimated using a Monte Carlo approach [*Zaehle et al.*, 2005]. Global simulations are conducted for 50 realizations of the parameter set (excepting V_{cmax}) by randomly selecting parameter values between their lower and upper observed limits. The standard deviation in predicted regional ET provides a measure of uncertainty for the global simulation. To drive the decadal global simulation under increasing atmospheric CO_2 concentration (phase 3) we adopt the 3-hourly Princeton meteorology [*Sheffield et al.*, 2006] covering the period 1948–2000. Phenology for the same period is reconstructed using an algorithm based on annual precipitation and average air temperature calibrated against satellite-derived LAI [*Los et al.*, 2006]. Atmospheric CO_2 concentration is adopted from the Law Dome ice core [*Etheridge et al.*, 1996] for 1948–1958 and from *Keeling et al.* [2009] for 1959–2000. For computational expediency, both the decadal simulation in phase 3 and the Monte Carlo uncertainty analysis from phase 2, are conducted at 3° spatial resolution. This produces global fluxes with 2–3% precision compared to 1° simulations [see also *Mueller and Lucht*, 2007].

2.2. Land Surface Modeling

[10] For the LSM, we adopt the Joint U.K. Land Environmental Simulator (JULES), which is an enhanced version of the Met Office land surface scheme (MOSES) [*Cox et al.*, 1999]. The energy calculation central to the model is based on a Penman-Monteith approach [*Monteith*, 1965]. An energy balance is conducted independently for each of 9 categories of surface cover (tiles) which make up any given landpoint. Tiles consist of five PFTs (broadleaf forest, needleleaf forest, C_3 grass, C_4 grass and shrub) and 4 nonvegetation tiles (urban, water, ice and bare ground). For global simulations, cover type at each landpoint, including the fraction of each PFT, is taken from the International Geosphere-Biosphere Project (IGBP) classification [*IGBP*, 1992; *Hansen and Reed*, 2000] which has been simplified to five PFTs for use with JULES and its predecessor MOSES [*Cox et al.*, 1999]. Surface albedo and the penetration of light into the canopy are estimated according to the two-stream formulation [*Sellers et al.*, 1996a, 1996b]. The latter is enhanced to take account of sunfleck penetration, explicit leaf orientation and the fraction of sunlight that is diffuse [*Alton et al.*, 2007b, 2007c]. Stomatal conductance, transpiration and leaf photosynthesis are calculated separately for each of 5 canopy layers, before summing to produce total values for the canopy [*Mercado et al.*, 2007; *Alton et al.*, 2007b]. Leaf C_3 and C_4 photosynthesis are derived using the colimitation model of *Collatz et al.* [1991], which is conceptually similar to the biochemical model of *Farquhar et al.* [1980]. We refer to *Alton et al.* [2005] for the equations governing leaf photosynthesis and the carbon model. Apart from meteorological driving data and phenology, input to the simulation occurs through a control file prescribing general and PFT-specific biophysical parameters. Values for these parameters are assigned according to average field measurements in the literature (see Text S1) except top-of-canopy photosynthetic capacity (V_{cmax}) which is tuned in order to make a straightforward calibration of the model.

[11] This study compares two schemes of plant hydrology implemented within JULES. A technical description of each scheme is given in the Accompanying Online material although the salient qualitative differences between the two schemes are summarized here. The first scheme uses the Ball-Berry relation [*Ball et al.*, 1987] to regulate stomatal conductance and a soil-moisture stress function which declines exponentially with decreasing soil moisture content. Stomatal conductance depends linearly on canopy humidity. This is the plant hydrology adopted in the Simple Biosphere model [*Sellers et al.*, 1996a, 1996b] and we refer to it as the SiB scheme hereafter. The second scheme is a more mechanistic approach based on the soil-plant-atmosphere (SPA) model of *Williams et al.* [1996]. SPA represents the processes which affect leaf water status. Stomata are opened incrementally until either the increase in leaf net carbon assimilation is less than a predetermined threshold or leaf water potential reaches a prescribed minimum value. The first condition assures control over plant water use efficiency (WUE) [*Cowan*, 1977; *Meinzer and Grantz*, 1991], whilst the threshold for leaf water potential prevents severe xylem cavitation [*Tyree and Sperry*, 1988]. Leaf water status is calculated explicitly according to the hydraulic resistance associated with extraction (i.e. resistance in the stem, roots and soil), the ability of the canopy to store water (capacitance) and the loss of water vapor through the stomata.

[12] Regardless of the plant hydrology scheme implemented in the LSM, we adopt the same biophysical parameters per PFT, including soil and root properties (see Text S1). Thus the simulations we conduct at both site level and globally vary only according to the plant hydrology scheme that is implemented. Within JULES, the soil moisture content is updated at each time step according to PPT, interception, throughfall, snowmelt, percolation, runoff and ET. Evapotranspiration comprises transpiration, soil evaporation and evaporation from water lying on plant surfaces (canopy surface water). Runoff consists of surface runoff and gravitational drainage from the lowest soil layer. Interception of rainfall is modeled as an exponential function of rainfall rate and the ratio of current to maximum canopy surface water [*Gregory and Smith*, 1990]. Maximum canopy surface water is proportional to LAI [*Ramirez and Senarath*, 2000]. Throughfall either percolates into the upper soil layer, according to an exponential function of rainfall rate [*Gregory and Smith*, 1990], or is routed to surface runoff. Moisture in the soil layers is extracted according to transpirational demand and the exponential distribution of the fine rootstock. Moisture is also lost from the upper soil layer as soil evaporation. Soil evaporation

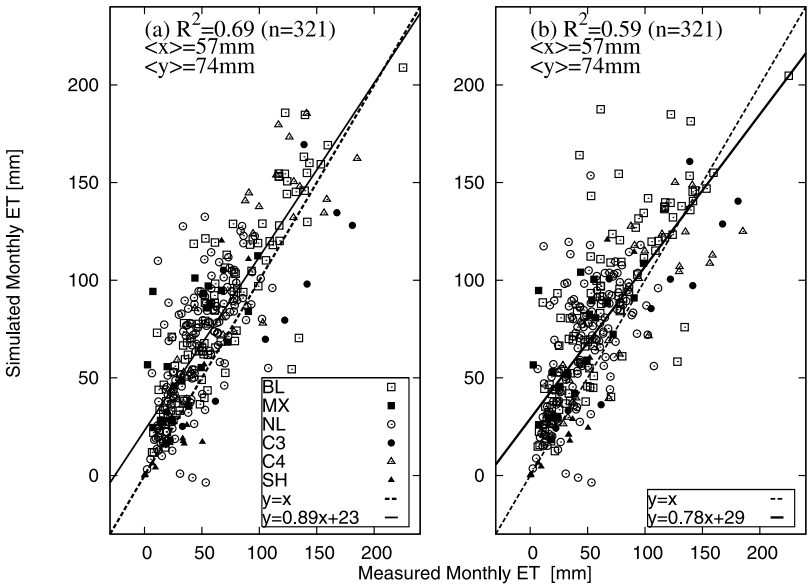

Figure 1. A comparison of simulated and measured monthly evapotranspiration (ET) at the Marconi sites. Simulations using the (a) SiB and (b) soil-plant-atmosphere (SPA) plant hydrology schemes. Also shown are the best-fit linear regression (solid line), the coefficient of determination (R^2), the observed mean ($\langle x \rangle$), the simulated mean ($\langle y \rangle$), the number of data (n), and the 1:1 relation (dashed line). For both linear fits, $p<0.01$. PFTs are broadleaf (BL), needleleaf (NL), C_3 grassland (C_3), C_4 grassland (C_4), and shrubs (SH).

varies according to vapor pressure deficit at the surface and the canopy aerodynamic resistance. It is also subject to a fixed soil surface resistance of 100 s m^{-1} [*Cox et al.*, 1999].

3. Results

3.1. Model Calibration and Validation (Phase 1)

[13] Both plant hydrology schemes yield similar calibrated values of photosynthetic capacity V_{cmax} (Table 5 of Text S1) which approximate field measurements fairly well [*Schulze et al.*, 1994; *Dang et al.*, 1998; *Carswell et al.*, 2000; *Lewis et al.*, 2000; *Meir et al.*, 2002]. To identify more readily behavioral differences between the SiB and SPA plant hydrology schemes, we adopt the average value from both schemes in order to calibrate each PFT within the global simulation, thus: 45, 43, 35, 13 and 21 μmol m^{-2} s^{-1} for BL, NL, C_3, C_4 and SH, respectively. With this calibration, global GPP (123–136 Gt yr^{-1}) lies in the middle of current model estimates (107–167 Gt yr^{-1}) [*Knorr and Heimann*, 2001; *Cramer et al.*, 2001] assuming a global NPP-to-GPP ratio of 0.42 [*Ruimy et al.*, 1996; *DeLucia et al.*, 2007].

[14] Both the SiB and SPA plant hydrology schemes predict monthly ET at the Marconi sites with a fair degree of success. Thus, using the median V_{cmax} for each PFT, the coefficient of determination (R^2) is 0.69 and 0.59 (n=321; $p<0.001$) for SiB and SPA, respectively (Figure 1). The same plot, using values of V_{cmax} calibrated separately for each site, reveals an almost identical level of correlation (R^2 = 0.70 and 0.57, respectively). Therefore, we focus on the median calibration hereafter. Growing season TR is predicted very successfully by both plant hydrology schemes (Figure 2), with R^2=0.90 and R^2=0.77 for SiB and SPA, respectively (n=7; $p<0.01$). The performance of the current schemes is typical of other LSMs predicting LE or surface water conductance [e.g., *Baldocchi and Harley*, 1995; *Misson et al.*, 2004]. Both plant hydrology schemes overestimate monthly ET and growing season TR by 30% on average. One possibility is that the Marconi observed fluxes underestimate ET and TR, despite our rejection of fluxes recorded under low airflow. Comparison of the annual net radiation recorded in the Marconi meteorology with the corresponding sum of latent and sensible heat yields 70% closure in the energy budget, which is in fair agreement with the 20% closure deficit estimated by *Wilson et al.* [2002] for a subset of the Marconi site years. Despite a general problem with closure, deficiencies with both plant hydrology schemes cannot be ruled out for certain parts of the growing season and the diurnal cycle. Overestimation of ET is greatest during the early part of the growing season when soil moisture content is highest (Figure 3). Furthermore, the SPA scheme overestimates ET during the morning whilst overestimation associated with the SiB scheme is more broadly distributed throughout the day. Despite differences in phase, the amplitude averaged across the diurnal cycle is similar in both models producing equivalent monthly ET in Figure 1.

3.2. Global Simulations (Phases 2 and 3)

[15] In stark contrast to the overestimation of site-level ET, both plant hydrology schemes generally underestimate zonal annual ET (Figure 4). Notably, tropical ET is underestimated by 25% (217 mm). However, caution is required when interpreting these results. Firstly, the simulations are subject to systematic errors owing to uncertainty in the model parameterization. For example, the uncertainty in ET

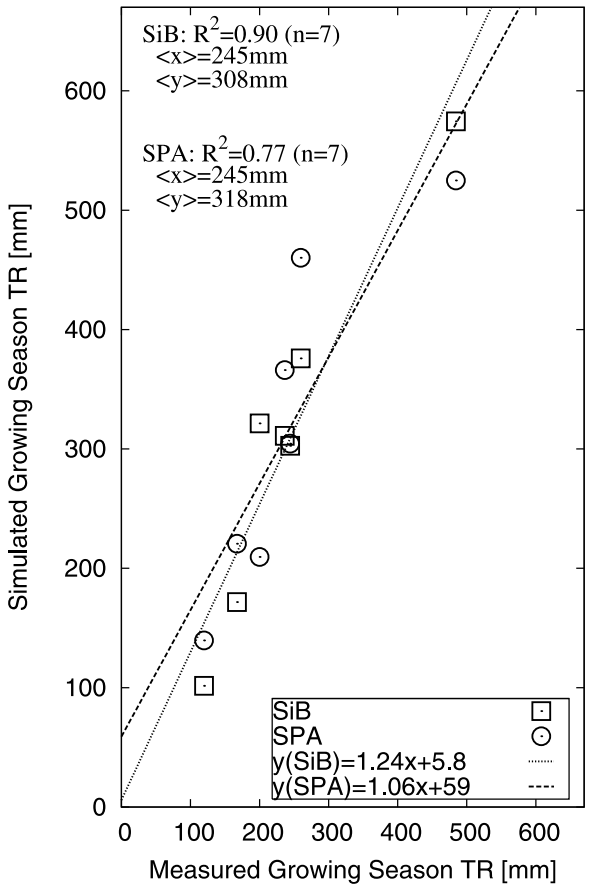

Figure 2. A comparison of simulated and measured growing season transpiration (TR) at the Marconi sites. Simulations are conducted separately using the SPA and SiB plant hydrology schemes. Measurements are derived previously from below-canopy eddy covariance fluxes [*Law et al.*, 2002] and the scaling of sap flow [*Granier et al.*, 2000; *Lundblad and Lindroth*, 2002]. Also shown are the best-fit linear regressions (dashed and dotted lines), the coefficient of determination (R^2), the observed mean ($\langle x \rangle$), the simulated mean ($\langle y \rangle$), and the number of site years (n). For all regressions, $p<0.01$.

is estimated as 13% using the Monte Carlo approach described in section 2.1. Secondly, estimates of zonal ET, used to validate the LSM, are themselves subject to significant uncertainties. For example, over the zonal range covering the vast majority of the Marconi sites (35°–70°), the model underestimates annual ET by 14% (44 mm) on average. However, it also underestimates runoff by 27% (75 mm) over the same latitudes (Figure 4). At least part of this inconsistency can be attributed to differences in estimated annual precipitation and the uncertainty in the extent of drainage basins, both of which are required to infer ET (precipitation minus runoff). Frequently, modeling is required to determine the extent of the watershed while interpolation is employed in regions containing few rain and river gauges [*Labat et al.*, 2004; *Dai et al.*, 2009]. Errors in measured river discharge and regional rainfall are estimated, respectively, as 15% [*Coe*, 2000] and 15–30% [*Adler et al.*, 2003; *Fisher*, 2007]. Finally, we note that the Marconi sites do not differ too radically from the corresponding latitude band in terms of mean annual measured ET and its standard deviation (350±140 mm and 280±140 mm, respectively).

[16] Predicted ET has a similar latitudinal distribution for both the SiB and SPA plant hydrology schemes. The ratio ET/PPT is greatest for arid and semiarid (Mediterranean) zones (Figure 5). The ratio TR/PPT shows more divergence between the two plant hydrology schemes. In particular, the SPA scheme predicts less annual TR for latitudes within 40° of the equator compared to SiB. For both schemes, the ratio TR/PPT is predicted to be quite constant across a broad range of latitudes. For example, using the SPA scheme, TR/PPT varies by ≤20% for the latitudinal band −30° to +30°, despite large changes in average climate, leaf area and vegetation type over this region (Figure 5). The relative

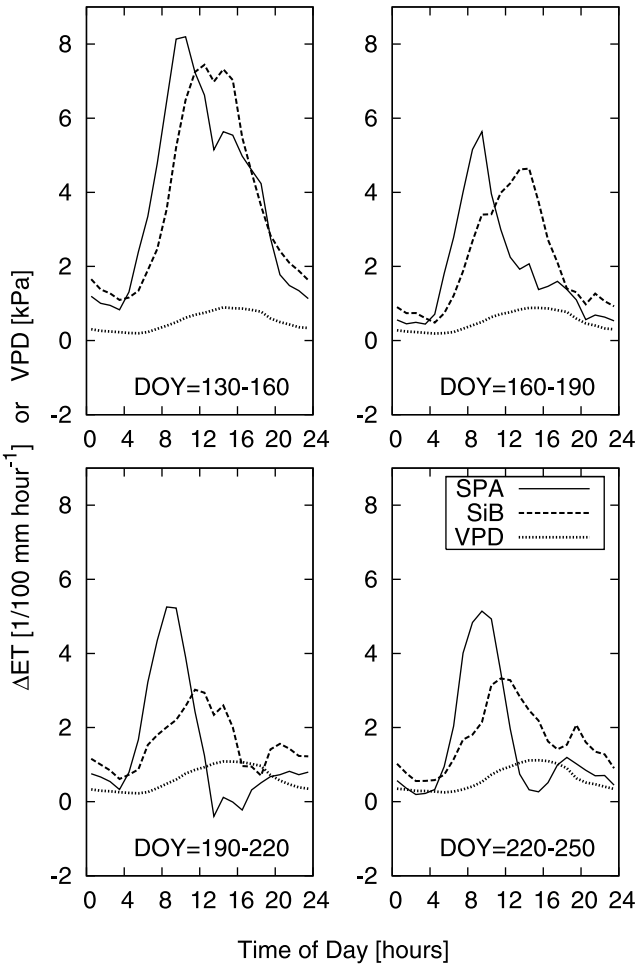

Figure 3. Simulated minus measured evapotranspiration (ΔET) in $\frac{1}{100}$ mm h^{-1}. Values are averaged over all site years for hourly bins of local time and for four periods of the growing season (DOY). A qualitatively similar response is exhibited by all PFTs before aggregation. ΔET is shown separately for both the SiB and SPA plant hydrology schemes. Vapor Pressure Deficit (VPD) in kPa is given by the dotted line.

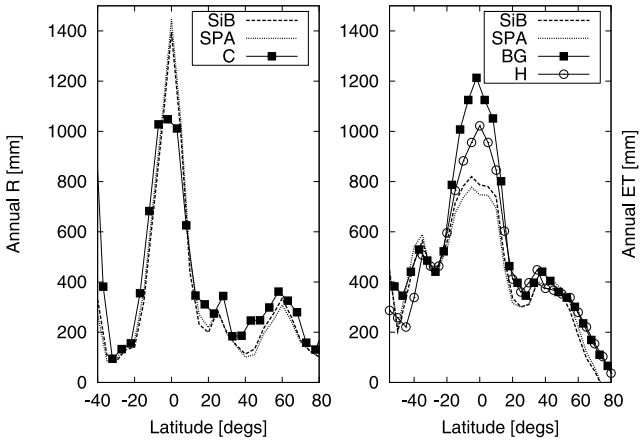

Figure 4. Latitudinal profiles of simulated and measured annual totals of evapotranspiration (ET) and annual runoff (R). Global simulations, forced by the GSWP meteorology (phase 2), are conducted separately using the SiB and SPA plant hydrology schemes. Runoff is measured by *Cogley* [2003] and denoted C. BG [*Baumgartner and Reichel*, 1975] and H [*Henning*, 1989] refer to ET derived by subtracting observed river discharge from precipitation. The systematic errors in simulated ET and runoff, owing to uncertainty in the parameterizations of the model, are estimated as 13% and 33%, respectively, using the Monte Carlo approach described in the main text (section 2.1).

constancy of TR/PPT within the model could be explained by the positive correlation we observe between the two forcing variables PPT and LAI (Figure 6). Any reduction in annually averaged LAI is likely to decrease predicted TR. This may act to conserve the ratio TR/PPT over quite a large range of vegetation types and climatic conditions. Thus, with the SPA scheme, the ratio TR/PPT varies by $\leq$0.05 (20%) over the five PFTs defined in the model (Table 1). With the SiB scheme, the corresponding dispersion is equally small ($\leq$0.04 or 17%) if C_4 grassland is excluded. Transpiration may be higher for C_4 grass due to its different photosynthetic pathway compared to the remaining PFTs.

[17] Within Table 1, global runoff fraction compares favorably with observation, despite a general underestimation of zonal runoff in Figure 4. PFT-specific ratios of ET/PPT are within 0.03–0.04 of the corresponding estimates made by *Choudhury et al.* [1998] using a plant hydrology scheme functionally similar to SiB. However, they exceed values estimated using a simple source/sink atmospheric model (0.2±0.1) [*Brubaker et al.*, 1993], although the latter, which interprets air moisture measurements, is known to significantly underestimate regional ET [*Eltahir and Bras*, 1996]. The hydrological ratios ET/PPT and TR/PPT in Table 1 are remarkably stable over the last 7 years of the 10 year simulation. Interannual variability is $\leq$0.02 and the average values in Table 1 are convergent within 0.01 when increasing the integration period from 1 to 7 years.

[18] Seasonally, TR can assume an even greater importance within the hydrological cycle than might be surmised from Table 1. For example, during the boreal growing season (Day of Year = 130–255), the SiB plant hydrology predicts a ratio TR/PPT of $\simeq$1 for the Siberian needleleaf forest and $\geq$0.5 for the eastern United States broadleaf forest (Figure 7). The corresponding ratios using the SPA plant hydrology scheme are somewhat lower (0.8 and 0.3, respectively) owing to a more conservative use of plant water compared to SiB (discussed below in section 4.2). The ratio TR/ET is $\simeq$0.7 for both regions during this period. For the forests in the Marconi archive with available transpirational rates (Figure 2), the TR/ET ratio averages 0.73±0.12 (n=7) integrated over the growing season. The ratio TR/PPT within Figure 7 also tends to be high for regions subject to summer drought, although values in some sparsely vegetated regions (e.g. North Africa) have to be interpreted carefully since both TR and PPT are small,

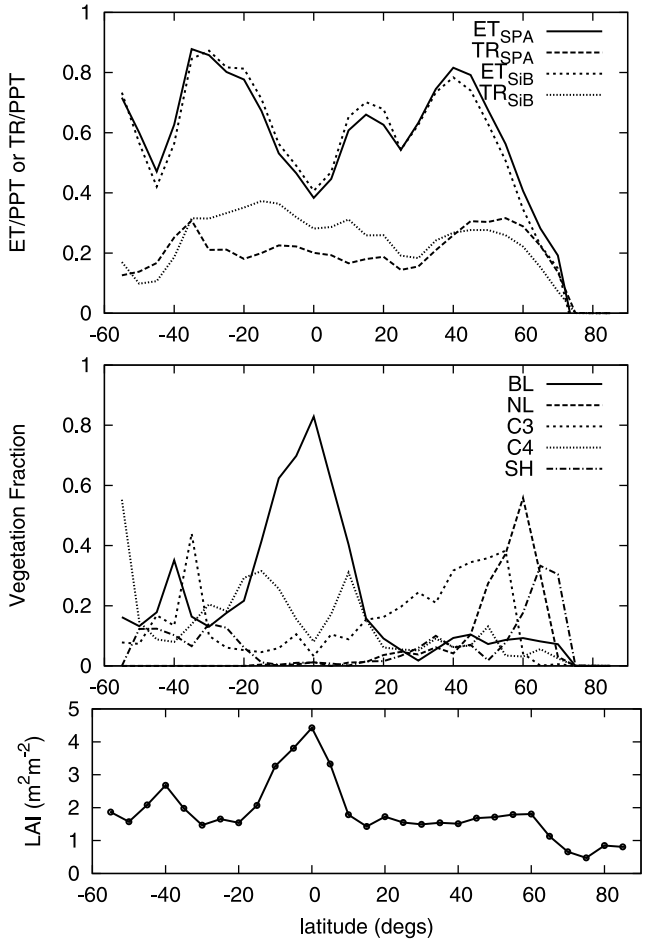

Figure 5. Latitudinal profiles of simulated annual evapotranspiration (ET) and transpiration (TR), shown as a proportion of annual precipitation (PPT), using the SiB and SPA plant hydrology schemes. (top) The systematic error in the ratios ET/PPT and TR/PPT, owing to uncertainty in the parametrization of the model, is estimated as 0.09 using the Monte Carlo approach described in the main text (section 2.1). (bottom and middle) For comparison, the annually averaged values of satellite-derived LAI and fraction of each vegetation type [*Los et al.*, 2000] are shown. Plant Functional Types are as designated in Figure 1.

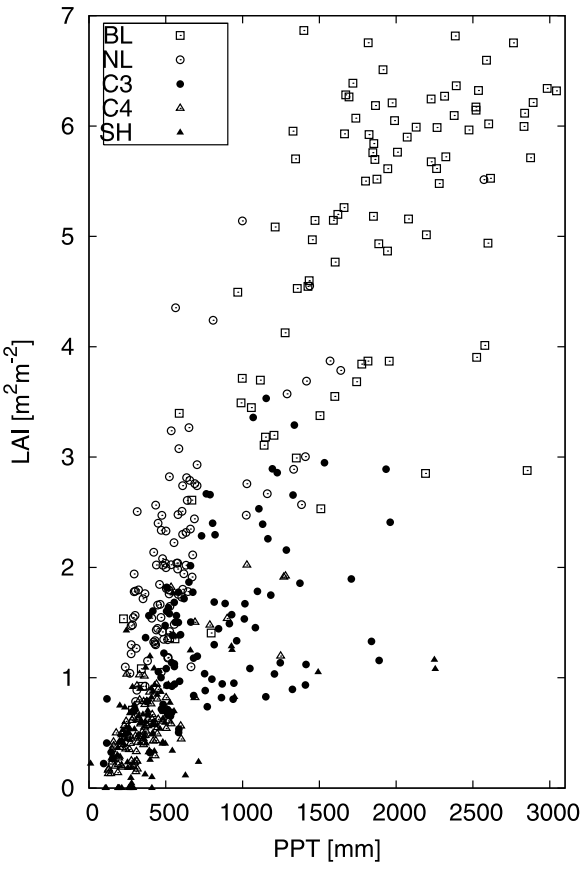

Figure 6. Annually averaged Leaf Area Index (LAI) against annual precipitation (PPT) for 500 global 1° landpoints (100 per PFT). Landpoints are covered by at least 75% of the appropriate vegetation type and are selected randomly from the global simulation. LAI is derived from satellite measurements of surface reflectance [*Los et al.*, 2000] whilst PPT is extracted from the GSWP reanalysis meteorology [*Dirmeyer et al.*, 1999].

making the metric TR/PPT unstable. Annual ecosystem water use efficiency (WUE; defined as the ratio GPP/ET) is similar for both plant hydrology schemes (Figure 8). Values are generally range from 3 for grasses to $\geq$ 8 for boreal conifers, in agreement with field measurements [*Law et al.*, 2002; *Ponton et al.*, 2006]. As discussed below, the high WUE associated with the northern conifer belt may relate to abundant soil moisture availability after the spring thaw and the relatively low vapor pressure deficit during the growing season.

[19] Both plant hydrology schemes suggest stability in the global hydrological cycle over the latter half of the 20th century (Figure 9). The predicted trend in global runoff (−1% over 50 years) agrees with recent estimates that sample 80% of the global runoff network (−1±2%) [*Dai et al.*, 2009]. Our simulations suggest that the trend and fluctuations in runoff are driven primarily by precipitation (correlation between the two variables of r^2=0.84; p<0.001). Fluctuations in precipitation relate strongly to the ENSO cycle [*Dai et al.*, 2009]. Although global trends in hydrological components over the 20th century are generally recognized as being small, regional changes in runoff and PPT can be quite pronounced [*Huntington*, 2006; *Dai et al.*, 2009].

4. Discussion

4.1. Global Distribution of Evapotranspiration

[20] The current study underlines the importance of TR in regional water and energy exchange. Globally, plants are responsible for returning $\simeq$ 25% of annual PPT to the atmosphere as transpiration. Seasonally, TR assumes an even greater role. During the northern hemisphere growing season, for example, TR is predicted to contribute two thirds of ET within the boreal conifer belt and the broadleaf forests of the eastern USA. For Siberia, TR is close to the amount of PPT occurring during this period. Thus whilst annual ET, as a fraction of PPT, increases slightly towards more arid latitudinal zones (Figure 5), vegetation appears to have a strong influence on the timing of water exchange between the land surface and the atmosphere, reclaiming water from the soil several months after it occurs as PPT and returning it to the atmosphere as TR. This is illustrated quite well by the boreal needleleaf forest where field measurements in Siberia confirm the rapid onset of photosynthesis and transpiration after the spring thaw [*Lloyd et al.*, 2002]. The boreal needleleaf forest typically benefits from a relatively low vapor pressure deficit during the growing season compared to grassland or broadleaf forest [*Ponton et al.*, 2006]. This leads to high values of both measured (Ponton et al.) and simulated (Figure 8) ecosystem WUE. Furthermore, the spring thaw should produce high values of soil moisture which is conducive to photosynthesis. We suggest caution in this interpretation since the spring is a highly transitional period for many environmental variables and biophysical properties including increased potential evapotranspiration and increased LAI [*Wilson and Baldocchi*, 2000; *Lawrence and Slingo*, 2004]. However, the steep rise in ET during the growing season is detected

Table 1. Annual Totals of Gross Primary Productivity, Evapotranspiration, Precipitation, Transpiration, and Aboveground and Belowground Runoff Simulated for Current and Recent Climate[a]

PFT	GPP	ET/PPT	TR/PPT	R/PPT	TR/ET	*n*
BL	58–64	0.49–0.50	0.24–0.33	0.51–0.53	0.49–0.65	2538
NL	17–19	0.45–0.51	0.26–0.31	0.49–0.54	0.58–0.61	1957
C_3	24–27	0.65–0.67	0.26–0.28	0.35–0.37	0.39–0.43	2364
C_4	20–21	0.68–0.73	0.21–0.44	0.29–0.34	0.32–0.60	1499
SH	4–5	0.49–0.53	0.22–0.27	0.43–0.46	0.44–0.51	1490
Global	123–136	0.58	0.22–0.28	0.43–0.44	0.38–0.48	15239

[a]Time period is 1989–1995. Values encompass the range predicted by both the SiB and soil-plant-atmosphere (SPA) plant hydrology schemes averaged over the 7 year period. In order to generate global totals, output from each 1° landpoint is assigned to one of the five Plant Function Types (PFTs) used in the model. PFTs are as designated in Figure 1. The equivalent number of landpoints is given by *n*. The systematic error in the ratios ET/PPT, TR/PPT, and R/PPT for each of the PFTs, owing to uncertainty in the parametrization of the model, is estimated as 0.09 using the Monte Carlo approach described in the main text (section 2.1). GPP, Gross Primary Productivity (Gt yr^{-1}); ET, evapotranspiration; PPT, precipitation; TR, transpiration; R, aboveground and belowground runoff.

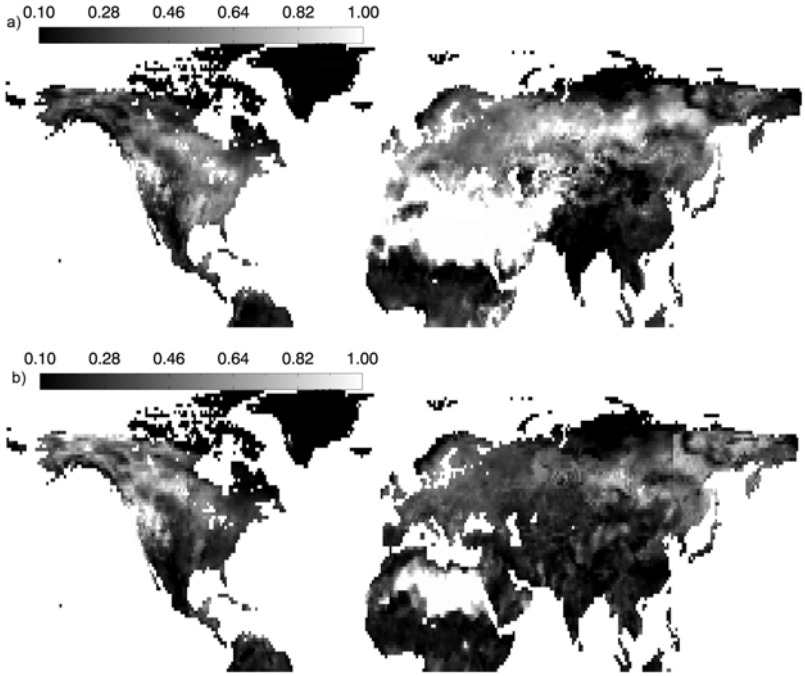

Figure 7. (a) The North Hemisphere ratio TR/PPT for transpiration (TR) and precipitation (PPT) integrated over days of the year 130–255. Transpiration is simulated using the SiB plant hydrology for landpoints of 1°. (b) As Figure 7a, but simulating transpiration using the SPA plant hydrology.

at site level by several authors, within a range of ecosystems, although the contribution of TR to ET is not always measured separately [e.g., *Shuttleworth*, 1988; *Sala and Tenhunen*, 1996; *Wilson and Baldocchi*, 2000; *Williams et al.*, 2004].

[21] The current investigation reveals one of the problems of scaling land surface calculations from site to global level. Compared to observational estimates, ET and TR are overestimated by 30% at the Marconi sites. However, both ET and runoff are underestimated, by 14% and 27%, respectively, over the zonal range which includes the vast majority of the Marconi sites (35°–70°). Inconsistencies of a similar magnitude are noted by *Hickler et al.* [2006] when scaling ET from site to regional level. Problems of scaling arise

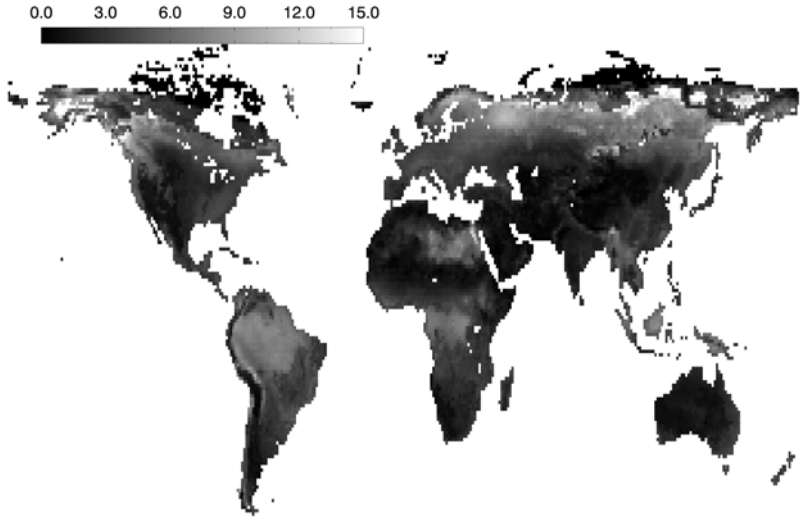

Figure 8. Global map of annual ecosystem water use efficiency (WUE; mmol mol^{-1}) simulated with the SiB plant hydrology scheme. The land surface model is forced by the GSWP reanalysis meteorology [*Dirmeyer et al.*, 1990]. The map has a spatial resolution of 1°, and WUE is averaged over a 7 year period. The corresponding simulation with the SPA plant hydrology scheme is very similar (RMS difference of ~0.5 mmol mol^{-1}).

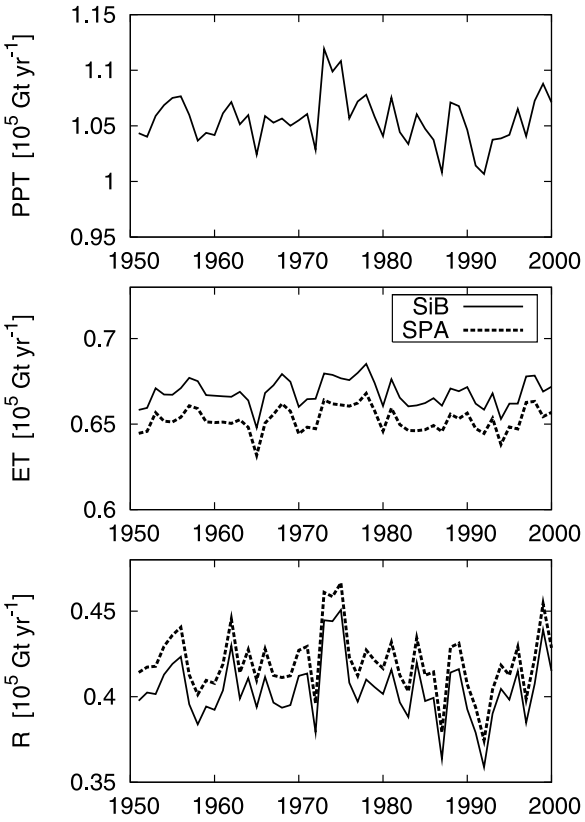

Figure 9. Global annual totals of (bottom) runoff (R) and (middle) evapotranspiration (ET) simulated using the SiB and SPA plant hydrology schemes for the latter half of the 20th century. (top) The corresponding annual precipitation (PPT). Values are in 10^5 gigatons (10^{17} kg).

from incomplete energy closure at FLUXNET sites [*Wilson et al.*, 2002], recovery from disturbance at calibration sites [*Friend et al.*, 2007] and significant differences (15–30%) in observational estimates of ET and runoff [*Coe*, 2000; *Adler et al.*, 2003; *Fisher*, 2007]. Indeed, the two observational estimates of zonal ET depicted in Figure 4 differ by more than the range predicted using the two schemes of plant hydrology. This suggests that there are some limitations to the extent to which observations can be used either to calibrate global LSMs or to discriminate between models in term of quality of output [see also *Zaehle et al.*, 2005]. It is also conceivable that the model scales poorly owing to systematic differences in meteorological or phenological forcing on different spatial scales [*Zhao et al.*, 2005]. For example, assuming systematic errors of 0.6–1.2 m^2 m^{-2} in LAI [*Gower et al.*, 1999; *Asner et al.*, 2003], we can account for one third of the 30% deficit in simulated ET at site level.

4.2. Uncertainties in Predicting ET Owing to Different Formulations of Plant Hydrology

[22] Despite quite different approaches offered by the SiB and SPA plant hydrology schemes, we obtain fairly similar results when calculating global TR. Thus, the global annual ratio TR/PPT is 0.22±0.09 and 0.28±0.09 using the SPA and SiB schemes, respectively. Regionally, the biggest difference occurs at latitudes near −20°, where C_4 grasses dominate. Overall, the SPA scheme appears to be more conservative with respect to plant water use efficiency compared to the SiB scheme. We can explain many of the differences in model behavior by the complete or partial closure of the stomata in SPA during the late morning when water stored in aboveground plant tissues becomes exhausted. Thereafter, moisture must be drawn from the soil and the increased resistance, associated with the soil, root and stem hydraulic pathway, act to limit TR. Within the SiB scheme no such storage is formulated and this represents a fundamental difference between the operation of the two schemes. In consequence, stomatal conductance during the morning may be higher in the SPA scheme but the stomata stay open longer in the SiB scheme making the plant more susceptible to water loss during the midafternoon when vapor pressure deficit is high (Figure 3). Plants are sometimes observed closing their stomata down during the warmest part of the day [*Roessler and Monson*, 1985; *Hirasawa and Hsiao*, 1999; *Jones*, 1992; *Franco and Luettge*, 2002] although it is not clear whether vegetation is reacting to leaf water potential (as in SPA), VPD (as in both SPA and SiB) or a circadian rhythm (neither SiB nor SPA).

[23] It is possible that the tuning of stomatal parameters to individual sites would remove some of the differences between predicted and observed ET evident over the diurnal cycle in Figure 3. However, this is unlikely to eliminate the problems of bias identified above i.e. overestimation of ET recorded at site level but underestimation of zonal ET. We believe that our current calibration procedure is mostly limited by the systematic errors within the observational data sets. We refer to *Alton and Bodin* [2009] for a more in-depth discussion of calibration issues.

[24] It is difficult to know whether our findings form part of a general difference between process-based plant hydrology schemes and more empirical methods. The process-based plant hydrology scheme implemented in LPJ [*Hickler et al.*, 2006] does not account for crown capacitance and, as such, cannot be compared directly with the SPA scheme of the current investigation. *Hunt et al.* [1991] recognize the fundamental difference between steady-state and non-steady-state models of plant water flow. The latter are characterized, as in the SPA scheme, by water storage (capacitance) terms which confer an advantage over steady-state models (such as the SiB scheme) when predicting instantaneous transpiration over the diurnal course. *Hunt et al.* [1991] argue that the difference between the two types of model is less important for daily totals of transpiration. Indeed, despite quite large divergences predicted by the SPA and SiB plant hydrology schemes over the diurnal course at the Marconi sites (Figure 3), annual values of ET and TR predicted for global PFTs, with the exception of C_4 grassland, are quite similar within both schemes (Table 1). Furthermore, annual values do not diverge significantly when both schemes are driven by increasing atmospheric CO_2 concentration and climate change (Figure 9).

4.3. Mechanistic or Empirical Approach to Plant Hydrology?

[25] With respect to plant hydrology, it worthwhile considering which of the currently developed methods are appropriate to global land surface simulations. The current tendency is for LSMs to adopt stomatal conductance schemes that are directly coupled to leaf photosynthesis [*Cox et al.*, 1998; *Yu et al.*, 2004; *Niyogi et al.*, 2009]. This replaces schemes like the *Jarvis* [1976] multiplicative approach which do not depend directly on leaf photosynthetic rate but rather on incident PAR, as well as other environmental variables [*Misson et al.*, 2004]. During the RICE and PILPS workshop, 14 different LSMs are categorized according to whether transpiration is formulated using a supply-demand approach, a resistance type model (Ohm's law) or an approach based purely on the availability of soil moisture [*Mahfouf et al.*, 1996]. The plant hydrology schemes implemented in the current study use elements from the first two of these categories. Global LSMs that rely heavily on satellite date include *Fisher et al.* [2007] and the MODIS algorithms for GPP and NPP [*Running et al.*, 2004; *Heinsch et al.*, 2006]. *Fisher et al.* [2007] predict monthly LE at 16 FLUXNET sites with $R^2 = 0.90$ using a modified Priestley-Taylor equation subject to 4 plant physiological limitations: LAI, green fraction, plant temperature and plant moisture. For each global landpoint, the 4 limitations follow from satellite data for such quantities such as absorbed PAR and NDVI. The model is remarkable for its skill in reproducing site-level LE without any form of calibration. The MODIS algorithm uses a productivity (light-use) efficiency approach which only accounts indirectly for soil moisture content through a linear dependency (via a ramp function) on daily vapor pressure deficit [*Coops et al.*, 2007].

[26] With the biophysical parameter values employed in the current investigation, there is no evidence that the SPA scheme performs any better than a traditional, less mechanistic approach based on the Ball-Berry stomatal model. This assertion is based on a comparison with measured ET at both site and regional level. Within the SPA scheme, the timing of stomatal closure, as discussed above, depends strongly on aboveground capacitance which, particularly for grasses and shrubs, is poorly known. In individual site studies of broadleaf forest, SPA reproduces very well the diurnal course of LE, stomatal conductance and leaf water potential using SPA [*Williams et al.*, 1996; *Fisher et al.*, 2006]. Parametrization and validation at individual sites, other than broadleaf forest, represents work in progress. Within the current investigation, the tendency for the SPA scheme to overestimate morning evapotranspiration might be explained by a lack of measured site-specific parameter values. As more field measurements of root resistance, capacitance and minimum leaf water potential become available for a greater range of vegetation types there will be potential for a more mechanistic approach to plant hydrology within global LSMs. Indeed, such an approach possesses obvious advantages compared to either empirical schemes or algorithms driven purely by satellite data [e.g., *Fisher et al.*, 2007]. For example, a mechanistic understanding of the physical processes by which plants release LE and moisture into the atmosphere becomes important when predicting the response of the land surface to future climate change.

5. Conclusions

[27] We implement a mechanistic scheme of plant hydrology (SPA) into a global LSM in order to compare with a more empirical plant hydrology scheme (SiB) that is traditionally adopted in global land surface simulations. Measured fluxes for 71 site years within the Marconi FLUXNET archive permit both calibration of the LSM and validation of the model at site level. Global simulations conducted with both plant hydrology schemes are compared to measurements of current zonal ET and runoff and to global runoff during the latter half of the 20th century. Our main conclusions are as follows:

[28] 1. Using both plant hydrology schemes the annually averaged global ratio ET/PPT is 0.58±0.9. The annually averaged global ratio TR/PPT is 0.22±0.09 and 0.28±0.08 using the SPA and SiB plant hydrology schemes, respectively. Seasonally, transpiration can assume a greater importance. For example, TR/PPT and TR/ET are estimated as $\simeq$1 and $\simeq$0.7, respectively, for the Siberian needleleaf forest during the boreal growing season.

[29] 2. The output from the two plant hydrology schemes typically differs less than the systematic errors associated with the different observational data sets (eddy covariance fluxes, continental runoff etc.) employed to calibrate and validate the LSM. This makes it difficult to compare the quality of model output from each of plant hydrology schemes. Both plant hydrology schemes behave similarly under climate change and the rise in atmospheric CO_2 concentration during the latter half of the 20th century.

[30] 3. The SPA scheme is more conservative than the SiB scheme with respect to plant water use. The former takes account of water stored in aboveground plant tissues. As this stored leaf water becomes exhausted during the morning, moisture must be drawn up from the soil and the increased hydraulic resistance limits afternoon transpiration in a manner consistent with observed site-level fluxes. Both plant hydrology schemes have a tendency to overestimate site-level ET early in the growing season.

[31] **Acknowledgments.** We thank the PIs and Co-Is of FLUXNET who make their data freely available to the ecological modeling community through the Marconi archive, namely, E. Falge, M. Aubinet, P. Bakwin, P. Berbigier, C. Bernhofer, A. Black, R. Ceulemans, A. Dolman, A. Goldstein, M. Goulden, A. Granier, D. Hollinger, P. Jarvis, N. Jensen, K. Pilegaard, G. Katul, P. Kyaw Tha Paw, B. Law, A. Lindroth, D. Loustau, Y. Mahli, R. Manson, P. Moncrieff, E. Moors, W. Munger, T. Meyers, W. Oechel, E. Schulze, H. Thorgeirsson, J. Tenhunen, R. Valentini, S. Verma, T. Vesala, and S. Wofsy.

References

Adler, R. F., et al. (2003), The version 2 Global Precipitation Climatology Project (GPCP) monthly precipitation analysis (1979–present), *J. Hydrometeorol.*, *4*, 1147–1167.

Alton, P., and P. Bodin (2009), A comparative study of a productivity (light-use) efficiency and a multilayer land-surface model over different spatial and temporal scales, *For. Agric. Meteorol.*, in press.

Alton, P., P. North, J. Kaduk, and S. Los (2005), Radiative transfer modeling of direct and diffuse sunlight in a Siberian pine forest, *J. Geophys. Res.*, *110*, D23209, doi:10.1029/2005JD006060.

Alton, P., L. Mercado, and P. North (2007a), A sensitivity analysis of the land-surface scheme JULES conducted for three forest biomes: Biophysical parameters, model processes, and meteorological driving data, *Global Biogeochem. Cycles*, *20*, GB1008, doi:10.1029/2005GB002653.

Alton, P., P. North, and S. Los (2007b), The impact of diffuse sunlight on canopy light-use efficiency, gross photosynthetic product and net ecosystem exchange in three forest biomes, *Global Change Biol.*, *13*, 776–787.

Alton, P., R. Ellis, S. Los, and P. North (2007c), Improved global simulations of gross primary product based on a separate and explicit treatment of diffuse and direct sunlight, *J. Geophys. Res.*, *112*, D07203, doi:10.1029/2006JD008022.

Asner, G., J. Scurlock, and J. Hicke (2003), Global synthesis of leaf area index observations: Implications for ecological and remote sensing studies, *Global Ecol. Biogeogr.*, *12*, 191–205.

Baldocchi, D., and P. Harley (1995), Scaling carbon dioxide and water vapour exchange from leaf to canopy in deciduous forest: II. Model testing and application, *Plant Cell Environ.*, *18*, 1157–1173.

Baldocchi, D., E. Falge, and L. Gu (2001), FLUXNET: A new tool to study the temporatl and spatial variability of ecosystem-scale carbon dioxide, water vapour and energy flux densities Bull, *Am. Meteorol. Soc.*, *82*, 2415–2434.

Ball, J., E. Woodrow, and J. Berry (1987), A model predicting stomatal conductance and its contribution to the control of photosynthesis under different environmental conditions, in *Progress in Photosynthesis Research*, edited by J. Biggins and M. Nijhoff, pp. 221–224, M. Nijhoff Publ., Dordrecht, Netherlands.

Baumgartner, A., and E. Reichel (1975), *Die Weltwasserbilanz*, R. Oldenburg, Munich, Germany.

Brubaker, K., D. Entekhabi, and P. Eagleson (1993), Estimation of continental precipitation recycling, *J. Clim.*, *6*, 1077–1089.

Carswell, F. E., P. Meir, E. V. Wandelli, L. C. M. Bonates, B. Kruijt, E. M. Barbosa, A. D. Nobre, J. Grace, and P. G. Jarvis (2000), Photosynthetic capacity in a central Amazonian rain forest, *Tree Physiol.*, *20*, 179–186.

Choudhury, B., N. DiGirolamo, J. Susskind, W. Darnell, S. Gupta, and G. Asrar (1998), A biophysical process-based estimate of global land surface evaporation using satellite and ancillary data: II. Regional and global patterns of seasonal and annual variations, *J. Hydrol.*, *205*, 186–204.

Coe, M. (2000), Modeling terrestrial hydrological systems at the continental scale: Testing the accuracy of an atmospheric GCM, *J. Clim.*, *13*, 686–704.

Cogley, J. G. (2003), *GGHYDRO: Global Hydrographic Data*, release 2.3, *Trent Tech. Note 2003-1*, Dept. of Geogr., Trent Univ., Peterborough, Ont., Canada.

Collatz, C., J. Ball, C. Grivet, and J. Berry (1991), Physiological and environmental regulation of stomatal conductance, photosynthesis and transpiration: A model that includes laminar boundary layer, *Agric. For. Meteorol.*, *54*, 107–136.

Coops, N., R. Jassal, R. Leuning, A. Black, and K. Morgenstern (2007), Incorporation of a soil water modifier into MODIS predictions of temperate Douglas-fir gross primary productivity: Initial model development, *Agric. For. Meteorol.*, *147*, 99–109.

Cowan, I. (1977), Stomatal behaviour and environment, *Adv. Bot. Res.*, *4*, 1176–1227.

Cox, P., C. Huntingford, and R. Harding (1998), A canopy conductance and photosynthesis model for use in a GCM land surface scheme, *J. Hydrol.*, *212*, 79–94.

Cox, P., R. Betts, C. Bunton, R. Essery, P. Rowntree, and J. Smith (1999), The impact of new land surface physics on the GCM simulation of climate and climate sensitivity, *J. Clim. Dyn.*, *15*, 183–203.

Cramer, W., et al. (2001), Global response of terrestrial ecosystem structure and function to CO_2 and climate change: Results from six dynamic global vegetation models, *Global Change Biol.*, *7*, 357–373.

Dai, A., and I. Fung (1993), Can climate variability contribute to the missing CO_2 sink?, *Global Biogeochem. Cycles*, *7*, 599–609.

Dai, A., T. Qian, and K. Trenberth (2009), Changes in continental freshwater discharge from 1948 to 2004, *J. Clim.*, *22*, 2773–2792.

Dang, Q., H. Margolis, and G. Collatz (1998), Parameterization and testing of a coupled photosynthesis-stomatal conductance model for boreal trees, *Tree Physiol.*, *18*, 141–153.

DeLucia, E., J. Drake, R. Thomas, and M. Gonzalez-Melers (2007), Forest carbon use efficiency: Is respiration a constant fraction of gross primary production?, *Global Change Biol.*, *13*, 1157–1167.

Dirmeyer, P., A. Dolman, and N. Sato (1999), The global soil wetness project: A pilot project for global land surface modelling and validation, *Bull. Am. Meteorol. Soc.*, *80*, 851–878. (Available at http://www.iges.org/gswp/)

Eltahir, E., and R. Bras (1996), Precipitation recycling, *Rev. Geophys.*, *34*, 367–378.

Etheridge, D., L. Steele, R. Langenfelds, R. Francey, J. Barnola, and V. Morgan (1996), Natural and anthropogenic changes in atmospheric CO_2 over the last 1000 years from air in Antarctic ice and firn, *J. Geophys. Res.*, *101*, 4115–4128.

Falge, E., et al. (2002), Phase and amplitude of ecosystem carbon release and uptake potential as derived from FLUXNET measurements, *Agric. For. Meteorol.*, *113*, 75–95.

Farquhar, G., S. von Caemmerer, and J. Berry (1980), A biochemical model of photosynthetic CO_2 assimilation in leaves of C_3 species, *Planta*, *149*, 78–90.

Fisher, B. (2007), Statistical error decomposition of regional-scale climatological precipitation estimates from the Tropical Rainfall Measuring Mission (TRMM), *J. Appl. Meteorol. Climatol.*, *46*, 791–813.

Fisher, J., D. Baldocchi, and L. Misson (2007), What the towers don't see at night: Nocturnal sap flow in trees and shrubs at two AmeriFlux sites in California, *Tree Physiol.*, *27*, 597–610.

Fisher, J., K. Tu, and D. Baldocchi (2008), Global estimates of the land-atmosphere water flux based on monthly AVHRR and ISLSCP-II data, validated at 16 FLUXNET sites, *Remote Sens. Environ.*, *112*, 901–919.

Fisher, R., M. Williams, R. Lobo do Vale, A. Lola da Costa, and P. Meir (2006), Evidence from Amazonian forests is consistent with isohydric control of leaf water potential, *Plant Cell Environ.*, *29*(2), 151–165.

Franco, A., and U. Luettge (2002), Midday depression in savanna trees: Coordinated adjustments in photochemical efficiency, photorespiration, CO_2 assimilation and water use efficiency, *Oecologia*, *131*, 356–365.

Friend, A., A. Stevens, R. Knox, and M. Cannell (1997), A process-based, terrestrial biosphere model of ecosystem dynamics (Hybrid v3.0), *Ecol. Modell.*, *95*, 249–287.

Friend, A., et al. (2007), FLUXNET and modelling the global carbon cycle, *Global Change Biol.*, *13*, 610–633.

Gat, J., and E. Matsui (1991), Atmospheric water balance in the Amazon Basin: An isotopic evapotranspiration model, *J. Geophys. Res.*, *96*, 13,179–13,188.

Gordon, W., J. Famiglietti, N. Fowler, T. Kittel, and K. Hibbard (2004), Validation of simulated runoff from six terrestrial ecosystem models: Results from VEMAP, *Ecol. Appl.*, *14*, 527–545.

Goulden, M., J. Munger, S. Fan, B. Daube, and S. Wofsy (1996), Measurements of carbon sequestration by long-term eddy covariance: Methods and a critical evaluation of accuracy, *Global Change Biol.*, *2*, 169–182.

Gower, S., C. Kucharik, and J. Norman (1999), Direct and indirect estimation of leaf area index, f_{APAR} and net primary production of terrestrial ecosystems, *Remote Sens. Environ.*, *70*, 29–51.

Granier, A., P. Biron, and D. Lemoine (2000), Water balance, transpiration and canopy conductance in two beech stands, *Agric. For. Meteorol.*, *100*, 291–308.

Gregory, D., and R. N. B. Smith (1990), Canopy, surface and soil hydrology. Unified model documentation paper 25, Meteorol. Off., Bracknell, U. K.

Hansen, M., and B. Reed (2000), A comparison of the IGBP DISCover and University of Maryland 1 km global land cover products, *Int. J. Remote Sens.*, *21*, 1365–1373.

Heinsch, F., M. Zhao, and S. Running (2006), Evaluation of remote sensing based terrestrial productivity from MODIS using regional tower eddy flux network observations, *IEEE Trans. Geosci. Remote Sens.*, *44*, 1908–1925.

Henning, D. (1989), *Atlas of the Surface Heat Balance of the Continents*, Gebrueder Borntraeger, Berlin.

Hickler, T., I. Prentice, B. Smith, and M. Sykes (2006), Implementing plant hydraulic architecture within the LPJ dynamic global vegetation model, *Global Ecol. Biogeogr.*, *15*, 567–577.

Hirasawa, T., and T. Hsiao (1999), Some characteristics of reduced leaf photosynthesis at midday in maize growing in the field, *Field Crops Res.*, *62*, 53–62.

Hunt, E., S. Running, and C. Federer (1991), Extrapolating plant water flow resistances and capacitances to regional scales, *Agric. For. Meteorol.*, *54*, 169–195.

Huntington, T. (2006), Evidence for intensification of the global water cycle: Review and synthesis, *J. Hydrol.*, *319*, 83–95.

International Geosphere-Biosphere Project (IGBP) (1992), *Improved Global Data for Land Applications*, *IGBP Global Change Rep. 20*, edited by J. R. G. Townshend, Int. Geosph. Biosph. Programme, Stockholm.

Jarvis, P. (1976), The interpretation of the variations in leaf water potential and stomatal conductance found in canopies in the field, *Philos. Trans. R. Soc. London, Ser. B*, *273*, 593–610.

Jones, H. (1992), *Plant and Microclimate*, Cambridge Univ. Press, Cambridge, U. K.

Keeling, R., S. Piper, A. Bollenbacher, and J. Walker (2009), Atmospheric CO2 records from sites in the SIO air sampling network, in *Trends: A*

Compendium of Data on Global Change, Carbon Dioxide Inf. Anal. Cent., Oak Ridge Natl. Lab., U.S. Dept. of Energy, Oak Ridge, Tenn.

Knorr, W., and M. Heimann (2001), Uncertainties in global terrestrial biosphere modeling: 1. A comprehensive sensitivity analysis with a new photosynthesis and energy balance scheme, *Global Biogeochem. Cycles*, *15, 207–225.*

Labat, D., Y. Godderis, J-L. Probst, and J-L. Guyot (2004), Evidence for global runoff increase relating to climate warming, *Adv. Water Resour.*, *27*, 631–642.

Law, B., et al. (2002), Environmental controls over carbon dioxide and water vapour exchange of terrestrial vegetation, *Agric. For. Meteorol.*, *113*, 97–120.

Lawrence, D., and J. Slingo (2004), An annual cycle of vegetation in a GCM. Part 1: Implementation and impact on evaporation, *Clim. Dyn.*, *22*, 87–105.

Lewis, J., R. McKane, D. Tingey, and P. Beedlow (2000), Vertical gradients in photosynthetic light response within an old-growth douglas-fir and western hemlock canopy, *Tree Physiol.*, *20*, 447–456.

Lloyd, J., O. Shibistova, and D. Zolotoukhine (2002), Seasonal and annual variations in the photosynthetic productivity and carbon balance of a central Siberian pine forest, *Tellus, Ser. B*, *54*, 590–610.

Los, S., N. Pollack, and M. Parris (2000), A global 9-yr biophysical land surface dataset from NOAA AVHRR data, *J. Hydrometeorol.*, *1*, 183–199.

Los, S. O., G. P. Weedon, P. R. J. North, J. D. Kaduk, C. M. Taylor, and P. M. Cox (2006), An observation-based estimate of the strength of rainfall-vegetation interactions in the Sahel, *Geophys. Res. Lett.*, *33*, L16402, doi:10.1029/2006GL027065.

Lundblad, M., and A. Lindroth (2002), Stand transpiration and sapflow density in relation to weather, soil moisture and stand characteristics, *Basic Appl. Ecol.*, *3*, 229–243.

Mahfouf, J.-F., C. Ciret, and A. Ducharne (1996), Analysis of transpiration results from the RICE and PILPS workshop, *Global Planet. Change*, *13*, 73–88.

Medlyn, B., D. Barrett, J. Landsberg, P. Sands, and R. Clement (2003), Conversion of canopy-intercepted radiation to photosynthate: Review of modelling approaches for regional scales, *Funct. Plant Biol.*, *30*, 153–169.

Medlyn, B., A. Robinson, R. Clement, and E. McMurtie (2005), On the validation of models of forest CO_2 exchange using eddy covariance data: Some perils and pitfalls, *Tree Physiol.*, *25*, 839–857.

Meinzer, F., and D. Grantz (1991), Coordination of stomatal hydraulic and canopy boundary layer properties: Do stomata balance conductances by measuring transpiration?, *Physiol. Plant*, *83*, 324–329.

Meir, P., et al. (2002), Acclimation of photosynthetic capacity to irradiance in tree canopies in relation to leaf N concentration and leaf mass per unit area, *Plant Cell Environ.*, *25*, 343–357.

Mercado, L., C. Huntingford, J. Gash, P. Cox, and V. Jogireddy (2007), Improving the representation of radiation interception and photosynthesis for climate model application, *Tellus, Ser. B*, *59*, 553–569.

Misson, L., J. Panek, and A. Goldstein (2004), A comparison of three approaches to modelling leaf gas exchange in annually drought-stressed ponderosa pine forests, *Tree Physiol.*, *24*, 529–541.

Monteith, J. L. (1965), Evaporation and environment, *Symp. Soc. Exp. Biol.*, *19*, 205–234.

Mueller, C., and W. Lucht (2007), Robustness of terrestrial carbon and water cycle simulations against variations in spatial resolution, *J. Geophys. Res.*, *112*, D06105, doi:10.1029/2006JD007875.

Nemani, R., M. White, P. Thornton, K. Nishida, S. Reddy, J. Jenkins, and S. Running (2002), Recent trends in hydrologic balance have enhanced the terrestrial carbon sink in the United States, *Geophys. Res. Lett.*, *29*(10), 1468, doi:10.1029/2002GL014867.

Niyogi, D., K. Alapaty, S. Raman, and F. Chen (2009), Development and evaluation of a coupled photosynthesis-based Gas Exchange Evapotranspiration Model (GEM) for mesoscale weather forecasting applications, *J. Appl. Meteorol. Climatol.*, *48*, 349–368.

Peylin, P., P. Bousquet, C. Le Qur, S. Sitch, P. Friedlingstein, G. McKinley, N. Gruber, P. Rayner, and P. Ciais (2005), Multiple constraints on regional CO_2 flux variations over land and oceans, *Global Biogeochem. Cycles*, *19*, GB1011, doi:10.1029/2003GB002214.

Ponton, S., et al. (2006), Comparison of ecosystem water-use efficiency among Douglas-fir forest, aspen forest and grassland using eddy covariance and carbon isotope techniques, *Global Change Biol.*, *12*, 294–310.

Ramirez, J., and Senarath (2000), A Statistical-dynamical parameterization of interception and land surface-atmosphere interactions, *J. Clim.*, *22*, 4050–4063.

Reichstein, M., J. Tenhunen, O. Roupsard, J.-M. Ourcival, S. Rambal, F. Miglietta, A. Peressotti, M. Pecchiari, G. Tirone, and R. Valentini (2003), Inverse modelling of seasonal drought effects on canopy CO_2/H_2O exchange in three Mediterranean ecosystems, *J. Geophys. Res.*, *108*(D23), 4726, doi:10.1029/2003JD003430.

Roessler, P., and R. Monson (1985), Midday depression of net photosynthesis and stomatal conductance in Yucca glauca. Relative contributions of leaf temperature and leaf-to-air water vapour concentration difference, *Oecologia*, *67*, 380–387.

Ruimy, A., G. Dedieu, and B. Saugier (1996), A diagnostic model of continental gross primary productivity and net primary productivity, *Global Biogeochem. Cycles*, *10*, 269–285.

Running, S., R. Nemani, F. Heinsch, M. Zhao, M. Reeves, and H. Hashimoto (2004), A continuous satellite-derived measure of global terrestrial primary production, *BioScience*, *54*, 547–560.

Sala, A., and J. Tenhunen (1996), Simulations of canopy net photosynthesis and transpiration in *Quercus ilex* under the influence of seasonal drought, *Agric. For. Meteorol.*, *78*, 203–222.

Salati, E., A. Dall'Olio, E. Matsui, and J. Gat (1979), Recycling of water in the Amazon Basin: An isotopic study, *Water Resour. Res.*, *15*, 1250–1258.

Schulze, E-D., F. Kelliher, C. Korner, J. Lloyd, and R. Leuning (1994), Relationships amoung maximum stomatal conductance, ecosystem surface conductance, carbon assimilation rate and plant nitrogen nutrition: A global ecology scaling exercise, *Annu. Rev. Ecol. Syst.*, *25*, 629–660.

Sellers, P., et al. (1996a), A revised land surface parameterization (SiB2) for atmospheric GCMs. Part I: Model formulation, *J. Clim.*, *9*, 676–705.

Sellers, P., S. Los, C. Tucker, C. Justice, D. Dazlich, G. Collatz, and D. Randall (1996b), A revised land surface parameterization (SiB2) for atmospheric GCMs. Part II: The generation of global fields of terrestrial biophysical parameters from satellite data, *J. Clim.*, *9*, 706–737.

Sellers, P., R. Dickinson, and D. Randall (1997), Modeling the exchanges of energy, water and carbon between continents and the atmosphere, *Science*, *275*, 502–509.

Sheffield, J., G. Goteti, and E. Wood (2006), Development of a 50-year high-resolution global dataset of meteorological forcings for land surface modelling, *J. Clim.*, *19*, 3088–3111.

Shuttleworth, W. (1988), Evaporation from Amazonian rainforest, *Proc. R. Soc. London, Ser. B*, *233*, 321–346.

Tian, H., et al. (1998), Effect of interannual climate variability on carbon storage in Amazonian ecosystems, *Nature*, *396*, 664–667.

Trenberth, K., L. Smith, Q. Taotao, A. Dai, and J. Fasullo (2007), Estimates of the global water budget and its annual cycle using observational and model data, *J. Hydrol.*, *8*, 758–769.

Tyree, M., and J. Sperry (1988), Do woody plants operate near the point of catastrophic xylem dysfunction caused by dynamic water stress?, *Plant Physiol.*, *88*, 574–580.

Wang, Y., R. Leuning, H. Cleugh, and P. Coppin (2001), Parameter estimation in surface exchange models using nonlinear inversion: How many parameters can we estimate and which measurements are most useful?, *Global Change Biol.*, *7*, 495–510.

Williams, D., et al. (2004), Evapotranspiration components determined by stable isotope, sap flow and eddy covariance techniques, *Agric. For. Meteorol.*, *125*, 241–258.

Williams, M., et al. (1996), Modelling the soil-plant-atmosphere continuum in a *Quercus-Acer* stand at Harvard Forest: The regulation of stomatal conductance by light, nitrogen and soil/plant hydraulic properties, *Plant Cell Environ.*, *19*, 911–927.

Wilson, K., and D. Baldocchi (2000), Seasonal and interannual variability of energy fluxes over a broadleaved, temperate deciduous forest in North America, *Agric. For. Meteorol.*, *100*, 1–18.

Wilson, K., et al. (2002), Energy balance closure at FLUXNET sites, *Agric. For. Meteorol.*, *113*, 223–243.

Yu, Q., Y. Zhang, Y. Liu, and P. Shi (2004), Simulation of the stomatal conductance of winter wheat in response to light, temperature and CO2 changes, *Ann. Bot.*, *93*, 435–441.

Zaehle, S., S. Sitch, B. Smith, and F. Hatterman (2005), Effects of parameter uncertainties on the modeling of terrestrial biosphere dynamics, *Global Biogeochem. Cycles*, *19*, GB3020, doi:10.1029/2004GB002395.

Zhao, M., F. Heinscha, R. Ramakrishna, B. Nemani, and S. Running (2005), Improvements of the MODIS terrestrial gross and net primary production global data set, *Remote Sens. Environ.*, *95*, 164–176.

P. Alton and S. Los, Geography Department, Swansea University, Singleton Park, Swansea SA2 8PP, UK. (p.alton@swansea.ac.uk)

R. Fisher, Department of Animal and Plant Sciences, University of Sheffield, Alfred Denny Bldg., Western Bank, Sheffield S10 2TN, UK.

M. Williams, School of Geosciences, University of Edinburgh, Room 220A, Crew Bldg., The King's Buildings, West Mains Rd., Edinburgh EH9 3JN, UK.